Optics Letters

Electromagnetic modeling of large subwavelength-patterned highly resonant structures

P. C. Chaumet,[1] G. Demésy,[1] O. Gauthier-Lafaye,[2,3] A. Sentenac,[1] E. Popov,[1] and A.-L. Fehrembach[1,*]

[1]Aix-Marseille Université, CNRS, Ecole Centrale Marseille, Institut Fresnel UMR 7249, 13013 Marseille, France
[2]CNRS, LAAS, 7 avenue du Colonel Roche, F-31400 Toulouse, France
[3]Université de Toulouse, LAAS, F-31400 Toulouse, France
*Corresponding author: anne-laure.fehrembach@fresnel.fr

Received 4 March 2016; revised 20 April 2016; accepted 20 April 2016; posted 22 April 2016 (Doc. ID 260441); published 12 May 2016

The rigorous modeling of large (hundreds of wavelengths) optical resonant components patterned at a subwavelength scale remains a major issue, especially when long range interactions cannot be neglected. In this Letter, we compare the performances of the discrete dipole approximation approach to that of the Fourier modal, the finite element and the finite difference time domain methods, for simulating the spectral behavior of a cavity resonator integrated grating filter (CRIGF). When the component is invariant along one axis (two-dimensional configuration), the four techniques yield similar results, despite the modeling difficulty of such a structure. We also demonstrate, for the first time to the best of our knowledge, the rigorous modeling of a three-dimensional CRIGF.

OCIS codes: (050.2770) Gratings; (050.6624) Subwavelength structures; (230.7408) Wavelength filtering devices; (310.2790) Guided waves; (260.5740) Resonance.

http://dx.doi.org/10.1364/OL.41.002358

Much progress has been made during the last decades concerning the numerical modeling of photonic components. Numerous commercial or free numerical codes are now available, allowing modeling of photonic nano-structures. Yet, the modeling of the long structures of several hundreds of wavelengths patterned at the sub-wavelength scale still remains a challenge. A typical example of such a structure is the cavity resonator integrated grating filter (CRIGF), composed of a central sub-wavelength grating flanked with Bragg gratings, engraved on a multilayer stack of dielectric and non magnetic materials. The central grating acts as an input/output coupler, allowing us to excite a guided mode of the stack through one diffraction order, while the Bragg gratings prevent the mode to spread outside the structure. The excitation of the mode creates an extremely narrow resonance peak in the reflectivity or transmittivity spectrum of the component; the Bragg reflectors provide a huge angular acceptance, as compared to the infinite coupler grating [1–3]. The CRIGFs are promising components for filtering, source emission control, and extended cavity lasers [4–6]. Yet, the CRIGFs are difficult to model, on one hand because of their dimensions, as the lengths of the components are at least 150 wavelengths, and the patternings are at the subwavelength scale, but also because they are extremely resonant. The first modeling was based on an approximate coupled mode theory [7]. The rigorous numerical calculations reported in the literature use the finite difference time domain (FDTD) method [2,4] and Fourier modal method (FMM, also known as RCWA) [8], applied to 2D structures only (invariant along one direction). No numerical modeling for a three-dimensional (3D) CRIGF has been reported yet, to the best of our knowledge. In this Letter, we first present a comparison between the reflection spectra obtained for a 2D CRIGF, made with four different methods: the FMM [9], the finite element method (FEM) [10,11], the discrete dipole approximation (DDA) [12], and the FDTD method [13]. The four methods are in very good agreement. Yet, all but DDA reach their limits in terms of calculation time and memory resources. Hence, in the second part of this Letter, we focus on the DDA and present the modeling of a 3D CRIGF. Our aim is to validate the different methods and to demonstrate the possibility to model a 3D CRIGF.

The structure under study, together with a description of its parameters, is represented in Fig. 1. It is composed of a central grating acting as a coupler, flanked with Bragg gratings, deposited on a waveguiding layer (silicon nitride, relative permittivity of 3.88, thickness of h_w) on a substrate (silica, relative permittivity of 2.13). All the media are lossless dielectric materials. The coupler grating and the Bragg gratings have the same depth h_g and are made of air and silica. The patterning is invariant in the y direction. The choice of the parameters has been made according to the following rules: the period of the Bragg grating d_B must be half that of the coupler grating d_G so that the coupler grating presents a resonance peak at a wavelength located in the bang gap of the Bragg grating; the width of the hole of the Bragg grating a_B must be one half of its period, ensuring the most efficient Bragg reflection. The phase shift δ allows movement of the peak across the range of wavelengths inside the bandgap of the Bragg grating. We chose a phase shift leading to a peak near the middle

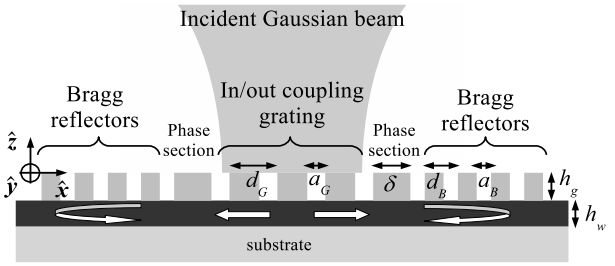

Fig. 1. Parameters of the test structure with 1D patterning (invariant along the y direction): $d_G = 480$ nm, $a_G = 240$ nm, $\delta = 360$ nm, $d_B = 240$ nm, $a_B = 120$ nm, $h_g = 120$ nm, and $h_w = 165$ nm. The relative permittivity of the substrate, waveguiding layer, and grating rectangular rods are 2.13, 3.88, and 2.13, respectively. The superstrate and grating holes are air. There are 200 Bragg periods on each side and 21 coupling grating periods.

of the Bragg bandgap, lying between 785.72 and 795.85 nm. (The calculation was done with our FMM code for an infinite Bragg grating replacing the CRIGF structuration in Fig. 1.) For the infinite coupler grating, the resonance peak is centered at 791 nm, and its width is 2.4 nm, tunable thanks to the hole width a_G. The number of Bragg grating periods is chosen to ensure a quasi-total reflectivity of the guided mode. The structure is modeled with four different methods: FMM, FEM, DDA, and FDTD. The FMM, FEM, and DDA represent homemade numerical codes, while the FDTD code is the freeware MEEP [13]. The four methods are based on different principles. The FMM, FEM, and DDA solve Maxwell harmonic equations, while the FDTD works in the time domain. The FEM, DDA, and FDTD compute the electromagnetic field in the direct domain, while it is the Fourier domain for the FMM.

The FMM has been developed to model infinite gratings periodic along two directions, with vertical walls. It was extended further on to model finite structures considered as the basic cell of a periodic structure and using absorbing layers or perfectly matched layers between each cell [14]. The application of the FMM to model CRIGF is presented in [8]. To model the structure of Fig. 1, 1401 Fourier orders (from −700 to 700) and 2.66 μm long absorbing layers were necessary. It is obvious that the large length of the structure increases a lot the calculation times of the scattering matrix as compared to smaller structures. Yet, on the other hand, we take advantage of the numerous diffraction orders of the structure to expand the incident Gaussian beam on these orders. Thus, we are able to calculate the response to a two-dimensional (2D) Gaussian beam (invariant along the y direction) with only one calculation of the scattering matrix per wavelength. The response to a 3D Gaussian beam is done by calculating the scattering matrix for several directions of the plane of incidence (from the (x, z) plane to the (y, z) plane) and for each plane, by expanding the beam on the numerous diffraction orders.

The main difficulty regarding the FEM formulation of the present problem relies on the choice of the unknown field that has to satisfy a proper outgoing wave condition. A relevant approach is to consider a planar reference structure composed of the guiding layer and substrate only (the grating is removed). The unknown field of our problem is then the difference between the total (incident and diffracted) field solutions of the diffraction problems when considering first the entire structure described in Fig. 1 and, second, the reference structure. In that way, the problem is reduced to the calculation of the field radiated by the set of rectangular rods of the structure put in the reference field. Standard Cartesian PMLs adapted to the substrate, superstrate, and guide were used to bind the computational domain and absorb the field radiated from the rods. Details can be found in [15]. Finally, the 2D Gaussian incidence is handled through a plane wave expansion, thus requiring, by virtue of the linearity of the Helmholtz operator, the resolution by the FEM only once per wavelength. The mesh element typical size used for the computation is $\lambda/(30)$ (where λ is the wavelength in the material), which typically ensures at least three significant digits upon energy related quantities. This problem has been implemented in practice into FEM softwares distributed under the terms of the GNU General Public License (GPL): Gmsh [16] for mesh generation and visualization, and GetDP [17] as a FEM library.

The DDA is a volume integral method based on the Green formalism [12,18]. The patterning is considered as a perturbation on a planar reference structure. The reference structure taken to model the CRIGF of Fig. 1 is the same as for the FEM (the substrate and the waveguiding layer). First, the area is discretized into cubic elements oriented along the x, y, and z axes. This allows us to model structures patterned along two orthogonal directions. Then the electric field inside the area is computed solving a very large linear system iteratively with the generalized product bi-conjugate gradient method with a residual error of 10^{-5} [19]. Second, the field diffracted by the structure is calculated using fast far-field calculation [20].

The reflection spectra calculated by the four methods are represented in Fig. 2. For the FMM, FEM, and FDTD, the

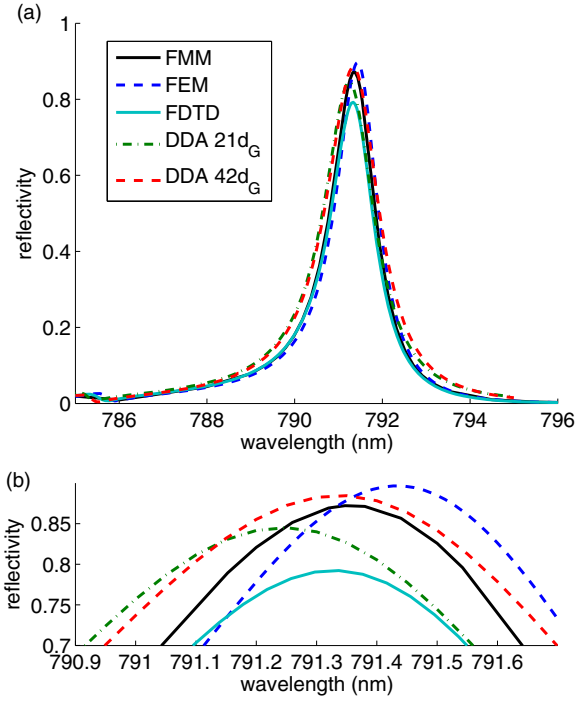

Fig. 2. (a) Comparison of the spectrum for the structure of Fig. 1 obtained with the FMM (black straight line), the FEM (blue dashed line), FDTD (cyan straight line), and the DDA for $21d_G$ (green dashed-dotted line), and $42d_G$ (red dashed line) along y. (b) Zoom-in on the top of the peak.

structure considered is invariant along the y axis while the calculation with the DDA is performed for a $21d_G$-long structure along y, $42d_G$-long and $63d_G$-long structures (superimposed with the $42d_G$ curve, not shown here). The incident beam is a normal incidence Gaussian beam with 10.36 μm diameter at the waist, which corresponds approximately to the beam waist maximizing the reflectivity at resonance. The Gaussian beam is invariant along the y direction for the FEM and FDTD (2D beam), while it is finite in the y direction (3D beam with axis having a circular symmetry of the field modulus) for the FMM and the DDA. It is polarized with an electric field in the (y, z) plane (s polarization).

We observe that the four methods are in very good agreement. It has to be noted that the calculation with the FMM with a Gaussian beam invariant along y gives a curve (not shown here) which coincides with the FEM curve, as if the higher reflectivity obtained with the FEM was due to the 2D Gaussian beam. On the other hand, the slightly lower reflectivity given by the FDTD method is due to the fact that it still has not fully converged, despite the use of a 2.5 nm grid resolution, illustrating the modeling difficulty of such resonant structures.

The possibility offered by the DDA to model a finite size structure along y allows us to study the effect of the size of the structure along this direction. It appears that a structuration twice as large as the coupling grating length is sufficient to ensure that the finite size has no impact on the reflectivity.

The larger spectral width obtained with the DDA may be due to a slower convergence with respect to the discretization step. The curve of Fig. 2 is calculated with a 60 nm step size. As shown in Fig. 3, a 120 nm step size gives a much larger peak centered at a smaller wavelength, while the peak obtained with a 40 nm step size is thinner than with a 60 nm step size, and nearly as thin as that obtained with the FMM.

The calculation time and the memory size required by the four methods are of the same order of magnitude (a few minutes per wavelength and a few gigabytes). Yet, with the FMM, FEM, and FDTD, the modeled structure is invariant along the y direction. We estimated that the modeling of the $42d_G$-long structure (whose size is 133 wavelengths along x and 25 wavelengths along y) would require 14 days per wavelength and more than 1800 GB for the FMM, 1000 days and 220 GB for the FDTD for the whole spectrum, and 14 h per wavelength and 2577 GB for the FEM, although it requires only 15 min per wavelength and 4 GB for the DDA.

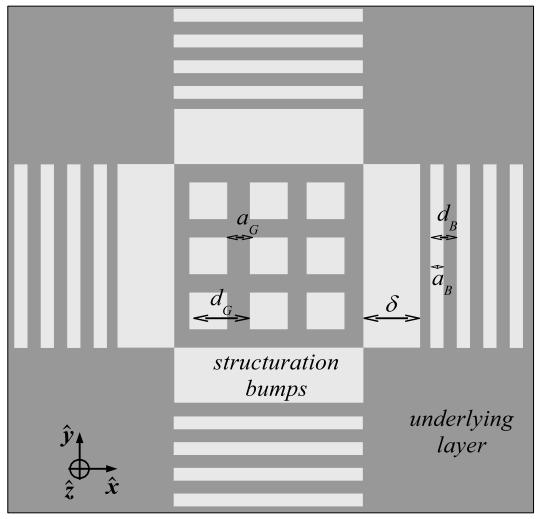

Fig. 4. Parameters of the structure studied with 2D patterning, top view (the layers below the grating are the same as for the structure of Fig. 1): $d_G = 480$ nm, $a_G = 120$ nm, $\delta = 120$ nm, $d_B = 240$ nm, and $a_B = 120$ nm. The patterning is the same along x and y. There are 200 Bragg periods on each side and 21 coupling grating periods.

In the following, we use the DDA only to model a 3D CRIGF. A 2D patterning with identical patterning along the two directions will ensure the independence of the spectrum with respect to the incident polarization under normal incidence. The parameters of the modeled structure are shown in Fig. 4. The parameters of the stack of layers and the grating thickness are the same as that of the 2D structure, and the period of the grating. The bump width was chosen so that the resonance peak obtained for the infinite coupler grating has a centering wavelength (790 nm) within the Bragg bandgap and a width bellow

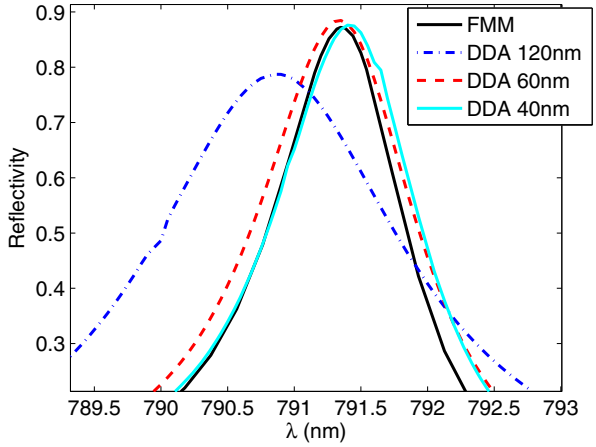

Fig. 3. Convergence of the DDA with respect to the step size: 120 nm (blue dashed-dotted line), 60 nm (red dashed line), and 40 nm (cyan straight line). The FMM curve (black straight line) is plotted for comparison.

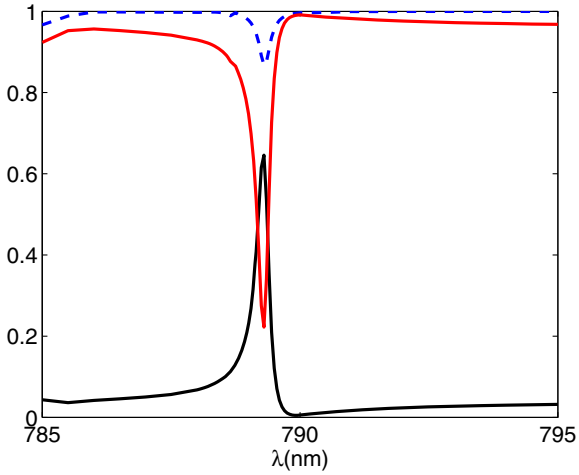

Fig. 5. Spectrum of the structure of Fig. 4 calculated with the DDA: reflectivity (black straight curve), transmittivity (red straight curve), and the sum of reflectivity and transmittivity (dotted blue curve).

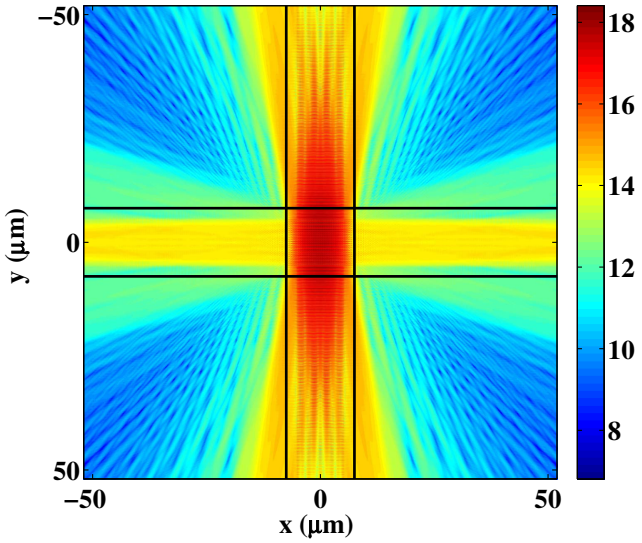

Fig. 6. Modulus of the electric field (incident plus reflected) for the structure of Fig. 4 at resonance ($\lambda = 789.3$ nm) calculated with the DDA. The color scale is logarithmic.

1 nm (0.57 nm). Each point of the spectrum needs one hour of computation with roughly 2×10^7 unknowns for the linear system to solve. (The code is not parallelized.)

The reflectivity (black straight curve), transmittivity (red straight curve), and the sum of reflectivity and transmittivity (dotted blue curve) with respect to the incident wavelength are presented in Fig. 5 for an incident electric field lying in the (x, z) plane. As expected, the same curve is obtained for the orthogonal polarization (not shown here). The Gaussian beam is 10.36 μm diameter at the waist, as for the 2D CRIGF. We also calculated the reflectivity for the same component but with $\delta = 360$ nm (instead of 120 nm). We obtained a peak centered almost at the same wavelength. This quasi-invariance of the peak position when the phase shift length is increased with the length of one period of the Bragg grating has already been observed for 2D CRIGF [2].

We observe in Fig. 5 that the reflectivity at resonance (64%) is smaller than for the 2D case, and that the losses reach 9%. As the media are lossless materials, the losses correspond to energy that escapes from the device through its edges. In Fig. 6, we show a map of the electric field in the (x, y) plane at resonance. The black straight lines show the outline of the Bragg and coupling gratings. The edges of the map are the edges of the device. We observe that the mode escapes out of the patterning at its entrance into the Bragg grating. In this Letter, we conclude that the laying out of the Bragg grating as shown in Fig. 4 is obviously not the most suitable to enhance the reflectivity at resonance. Bragg grating presenting, for example, a circular shape, as was done experimentally in [21], may be more suitable.

To sum up, we applied four numerical methods based on four different principles (F modal method, FEM, FDTD method, and DDA method) to calculate the reflectivity spectrum of a 2D CRIGF (invariant along one direction). The comparison shows an excellent agreement, thus validating the four methods for the modeling of 2D CRIGF. While these four methods (and probably other numerical methods not considered here) are able to tackle the 2D CRIGF problem, the DDA is the only one (among the four methods presented here) able to treat the 3D CRIGF. We believe that the possibility to model 3D CRIGF opens the way to numerous numerical studies, which are necessary to make the best design of 3D CRIGF (for applications requiring polarization independent components, for instance), or even 2D CRIGF taking into account the finite size effects.

Funding. Agence Nationale de la Recherche (ANR); Direction Générale de l'Armement (DGA); ASTRID program.

REFERENCES

1. K. Kintaka, T. Majima, J. Inoue, K. Hatanaka, N. Junji, and S. Ura, Opt. Express **20**, 1444 (2012).
2. X. Buet, E. Daran, D. Belharet, F. Lozes-Dupuy, A. Monmayrant, and O. Gauthier-Lafaye, Opt. Express **20**, 9322 (2012).
3. T. Kondo, S. Ura, and R. Magnusson, J. Opt. Soc. Am. A **32**, 1454 (2015).
4. Y. Zhou, M. Moewe, J. Kern, M. C. Y. Huang, and C. J. Chang-Hasnain, Opt. Express **16**, 17282 (2008).
5. K. Kintaka, Y. Kita, K. Shimizu, H. Matsuoka, S. Ura, and J. Nishii, Opt. Lett. **35**, 1989 (2010).
6. X. Buet, A. Guelmani, A. Monmayrant, S. Calvez, F. Lozes-Dupuy, and O. Gauthier-Lafaye, in *15th International Conference on Transparent Optical Networks (ICTON)*, Cartagena, 2013, paper We.B2.2.
7. S. Ura, S. Murata, Y. Awatsuji, and K. Kintaka, Opt. Express **16**, 12207 (2008).
8. N. Rassem, E. Popov, and A.-L. Fehrembach, Opt. Quantum Electron. **47**, 3171 (2015).
9. L. Li, J. Opt. Soc. Am. A **14**, 2758 (1997).
10. J.-M. Jin, *The Finite Element Method in Electromagnetics* (Wiley, 2014).
11. J.-C. Nédélec, Numer. Math. **35**, 315 (1980).
12. B. Draine, Astrophys. J. **333**, 848 (1988).
13. A. F. Oskooi, D. Roundy, M. Ibanescu, P. Bermel, J. D. Joannopoulos, and S. G. Johnson, Comput. Phys. Commun. **181**, 687 (2010).
14. E. Silberstein, P. Lalanne, J.-P. Hugonin, and Q. Cao, J. Opt. Soc. Am. A **18**, 2865 (2001).
15. G. Demésy, F. Zolla, A. Nicolet, M. Commandré, and C. Fossati, Opt. Express **15**, 18089 (2007).
16. C. Geuzaine and J.-F. Remacle, Int. J. Numer. Meth. Eng. **79**, 1309 (2009).
17. P. E. A. Dular, IEEE Trans. Magn. **34**, 3395 (1998).
18. P. C. Chaumet, A. Sentenac, and A. Rahmani, Phys. Rev. E **70**, 917 (2004).
19. P. C. Chaumet and A. Rahmani, Opt. Lett. **34**, 917 (2009).
20. P. C. Chaumet, T. Zhang, and A. Sentenac, J. Quant. Spectrosc. Radiat. Transfer **165**, 88 (2015).
21. K. Kintaka, T. Majima, K. Hatanaka, J. Inoue, and S. Ura, Opt. Lett. **37**, 3264 (2012).